Distributed Event-Triggered Control Strategy Based on Adaptive V-I Droop Characteristic for Accurate Load Sharing in AC Microgrids

Sadegh Golsorkhi, Mohammad; Hajian, Masoud; Savaghebi, Mehdi

Published in:
Proceedings of 2022 IEEE 13th International Symposium on Power Electronics for Distributed Generation Systems (PEDG)

Link to article, DOI:
10.1109/PEDG54999.2022.9923303

Publication date:
2022

Document Version
Peer reviewed version

Citation (APA):
Sadegh Golsorkhi, M., Hajian, M., & Savaghebi, M. (2022). Distributed Event-Triggered Control Strategy Based on Adaptive V-I Droop Characteristic for Accurate Load Sharing in AC Microgrids. In *Proceedings of 2022 IEEE 13th International Symposium on Power Electronics for Distributed Generation Systems (PEDG)* IEEE. https://doi.org/10.1109/PEDG54999.2022.9923303

Distributed Event-Triggered Control Strategy Based on Adaptive V-I Droop Characteristic for Accurate Load Sharing in AC Microgrids

Mohammad Sadegh Golsorkhi
Centre for Industrial Electronics,
Department of Mechanical and
Electrical Engineering, University of
Southern Denamark, Sønderborg,
Denmark
https://orcid.org/0000-0003-0408-729X

Masoud Hajian
Department of Electrical and Computer
Engineering, Isfahan university of
technology, Isfahan, Iran
masoudhajian@alumni.iut.ac.ir

Mehdi Savaghebi
Department of Engineering
Technology, Technical University of
Denmark, DK-2750 Ballerup, Denmark
https://orcid.org/0000-0001-6188-0265

Abstract— **This paper presents a new distributed event-triggered control mechanism for accurate load sharing and voltage regulation in islanded AC microgrids (MGs). The control structure is composed of two layers. The primary control level coordinates the output current of the Distributed Energy Resources (DERs) by utilizing the V-I droop control strategy. In this method, all DERs are synchronized to a common rotating reference frame. To realize proportional load sharing among the DERs, for each DER, the d and q components of the output voltage are determined in accordance to droop characteristics of the d and q axis currents. To eliminate the load sharing caused by the line voltage drops, the slope of the droop characteristic of each DER is altered by means of a distributed secondary control scheme. The secondary controller utilizes an event-triggered communication strategy, which remarkably decreases the exchanged data and saves bandwidth. Simulation results show that the proposed method favors smooth dynamic performance and efficient network utilization.**

Keywords— **microgrid, droop control, distributed control, event-triggered control.**

I. INTRODUCTION

Over the recent years, the concept of microgrid (MG) has attracted the attention of researchers and engineers as a systematic solution for integrating the Distributed Energy Resources (DERs) in distribution networks. The stable and reliable operation of MGs depends on coordinated control of DERs. Especially, during the islanded operation mode of MGs, the DERs are responsible for load/generation balance as well as voltage and frequency control [1]. Many different control strategies, including decentralized, centralized, and distributed approaches have been suggested for the control and coordination of DERs. In the decentralized method, DERs are controlled by local controllers, which are usually droop controllers. To tackle the limitations of the decentralized method, communication-based control methods including centralized and distributed control have been introduced. In the centralized approach, the DERs are coordinated through a central controller which provides the set points for DERs controllers. The central control scheme is costly in terms of communication network and suffers from a single point of failure [2]. To overcome the limitations of the centralized control scheme, distributed control structure has been proposed in the literature [3], [4]. In this approach, each DER is regarded as a control agent. The agents are interconnected via a sparse cyber network. By employing consensus protocol, the distributed controller corrects the error in power sharing associated with the primary control level and restores the voltage and frequency deviations caused by the droop characteristics. In [5], a distributed optimal control in suggested to improve the stability and minimize the generation cost. In [6], a droop-free distributed control is proposed for AC microgrids to share active and reactive power and control frequency. In the mentioned distributed control schemes, the majority of the data exchanged through the communication links are redundant, which results in excessive communication burden. To utilize the communication network more efficiently and reduce the number of controller updates, event-triggered strategies could be employed. In[7], an event-triggered secondary control with network delay has been proposed, and the primary level is comprised of Q-f and P-U droop characteristics. Reference [8] presents a decentralized event-triggered control to reduce the communication burden and restore voltage and frequency to nominal values. In [9], a centralized and distributed event-triggered control has been suggested to keep the frequency within the nominal range and compensate for the voltage deviations caused by the primary controller. In [10], a Zeno-free event-triggered strategy is suggested to achieve accurate power sharing and control voltage and frequency. In [11], authors review the recent advances in the event-triggered strategy and discuss different event-triggered approaches in detail. [9] presents a new event-triggered approach to reduce communication and exchanged data and to achieve distributed load sharing in an inverter-based microgrid. In [11], a distributed event-triggered control is proposed to keep frequency and voltage stable and achieve power sharing in an inverter-based microgrid.

In this paper, a new two-level control strategy is presented. In contrast with the existing event-triggered control schemes, which are based on the conventional P-f and Q-V droop control methods, the proposed scheme employs a V-I droop control strategy [12] in the primary control level. In this method, the DERs are synchronized to a common synchronous rotating reference frame and load sharing is realized through drooping the d and q components of the output voltage with the respective components of the current. This way, the problems of active and reactive power sharing are simplified to d and q axis current sharing. The distributed secondary controller alters the slope of d and q axis V-I droop characteristics of each DER such that the error in current sharing is eliminated. The data exchange among the DERs is controlled by an event-triggered algorithm. Simulation results show that the proposed control strategy avails accurate load sharing with smooth dynamic response and features significantly reduced communication network traffic.

The rest of the paper is organized as follows: Sections II and III discuss the primary and secondary controllers respectively. In section IV, the proposed event-triggered controller is proposed. Finally, the simulation results and conclusion are presented in Sections V and VI respectively.

II. PROPOSED CONTROL STRUCTURE

A. Control layout

Consider the islanded MG of Fig. 1, which is comprised of a number of DERs and loads connected through a low voltage distribution grid. Stable and reliable operation of the MG requires coordinated control of the DERs. Specifically, the DERs must be able to maintain voltage and frequency regulation while meeting the active and reactive power demand [13]. Furthermore, the load must be shared among the DERs according to their available capacity [14]. To meet these goals, a two-level control structure is proposed in this paper. The primary control level provides load sharing with fast dynamic response but lacks load sharing accuracy. To eliminate the error in load sharing among the DERs, the secondary control level is added on top of the primary level. The secondary control level employs a distributed structure and realizes accurate load sharing based on consensus protocol. The distributed control scheme is realized by interconnecting the DERs through a sparse communication network (shown with dashed lines in Fig. 1), which enables sharing of each DER's information with its neighbors.

B. Primary control level

Conventionally, P-f and Q-V droop controllers are used for synchronization and coordinated control of DERs in the primary layer. This control strategy relies on the assumption that the network impedance has a high X/R ratio, hence the active and reactive power output of each DER are proportional to the voltage angle (frequency) and magnitude, respectively. Nonetheless, this assumption is invalid in MGs, with the lines having a small X/R ratio.

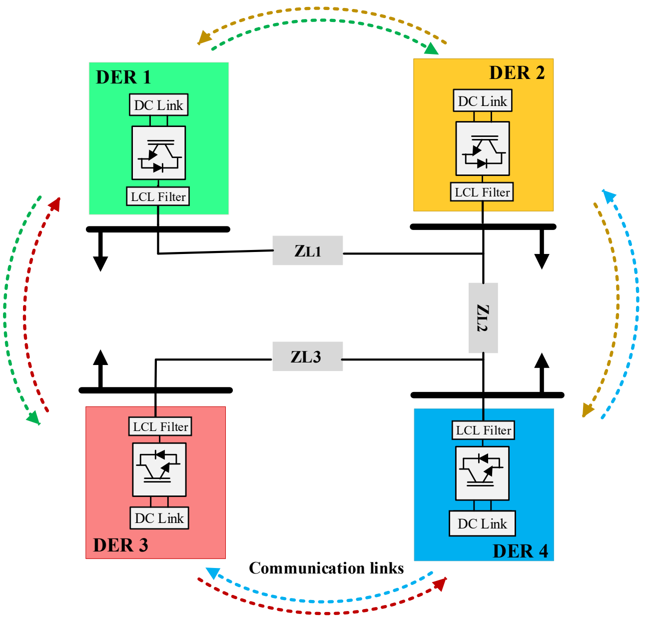

Fig. 1. Schematic diagram of an islanded MG with four DERs

To avoid the aforementioned issues, an alternative droop control scheme was proposed in [15] to achieve a fast dynamic response in terms of power sharing while realizing fixed frequency operation in islanded MGs. In this scheme, fixed frequency operation is realized by adopting the GPS time synchronization strategy. To that end, the local time of each DER is synchronized to the Universal Coordinated Time (UTC) using GPS timing technology. Such time coordination enables synchronization of the DER controllers to a global rotating reference frame, the angular frequency of which is fixed at the rated grid frequency [16]. In this frame the voltage of i^{th} DER is calculated based on the output current, as follows:

$$\begin{bmatrix} v_{di} \\ v_{qi} \end{bmatrix} = \begin{bmatrix} E_0 \\ 0 \end{bmatrix} - \begin{bmatrix} r_{di} & 0 \\ 0 & r_{qi} \end{bmatrix} \begin{bmatrix} i_{di} \\ i_{qi} \end{bmatrix} \tag{1}$$

in which v_d, v_q, i_d, i_q, r_d, r_q, and E_0 are the d and q axis components of the DER reference voltage, current, and virtual impedance and rated voltage.

C. Secondary Control level

As mentioned above, the droop controller causes voltage deviation and inaccurate current sharing. To achieve accurate current sharing, a secondary controller is adopted to modify the q- and d-axis components of virtual impedances of (1). Therefore (1) could be rewritten as:

$$\begin{bmatrix} v_{di} \\ v_{qi} \end{bmatrix} = \begin{bmatrix} E_0 \\ 0 \end{bmatrix} - \begin{bmatrix} r_{di}(t) & 0 \\ 0 & r_{qi}(t) \end{bmatrix} \begin{bmatrix} i_{di} \\ i_{qi} \end{bmatrix} + \begin{bmatrix} V_{sdi} \\ 0 \end{bmatrix} \tag{2}$$

where $r_{di}(t)$ and $r_{qi}(t)$ are defined as:

$$r_{di}(t) = r_{do} + \delta_{di}(t) \tag{3}$$

$$r_{qi}(t) = r_{qo} + \delta_{qi}(t) \tag{4}$$

$\delta_{di}(t)$, $\delta_{qi}(t)$, r_{do} and r_{qo} are d-axis current sharing correction term, q-axis current sharing correction term d-axis initial slope, and q-axis initial slope. As discussed earlier, droop controllers cause current mismatch among DERs. To resolve this problem, the slopes q- and d-axis components of virtual impedances are modified so as to mitigate this mismatch and acquire accurate current sharing.

To restore voltage to the nominal value, a voltage correction term (V_{sdi}) is added to the right-hand side of (1). V_{sdi} is defined as:

$$v_{sd,i} = \frac{k_v}{s}(E_0 - \bar{v}_i) \tag{5}$$

where k_v is the control gain and $\bar{v}_i$ is the average MG voltage across the DER buses estimated by unit *i*, which is obtained by the equation below:

$$\bar{v}_i = v_i + \frac{k_{avg}}{s}\sum_{j\in N_i} \bar{v}_j - \bar{v}_i \tag{6}$$

where k_{avg} is the control gain, N_i is the set of agent *i* neighbors, and v_i is the terminal voltage of agent *i*.

The problem of proportional load sharing is divided into proportional sharing of d-axis and q-axis currents. In the context of consensus control, the proportional sharing of d-axis current is equal to force the per unit d-axis current of each DER to reach a common value, which means:

$$\frac{i_{d,1}}{i_{d,1}^{rated}} = \frac{i_{d,2}}{i_{d,2}^{rated}} = \dots = \frac{i_{d,i}}{i_{d,i}^{rated}} \tag{7}$$

where $i_{d,i}^{rated}$ refers to the rated d-axis current of DER *i*. To achieve (7), d-axis virtual impedance is updated according to the difference between per unit d-axis currents of unit *i* and its neighbors as

$$r_{di}(t) = r_{do} + \frac{k_d}{s}\sum_{j\in N_i}\left(\frac{i_{d,j}}{i_{d,j}^{rated}} - \frac{i_{d,i}}{i_{d,i}^{rated}}\right) \tag{8}$$

in which s is the derivative operator and k_d is the integral gain.

Likewise, the q-axis virtual impedance is updated as

$$r_{qi}(t) = r_{qo} + \frac{k_q}{s}\sum_{j\in N_i}\left(\frac{i_{q,j}}{i_{q,j}^{rated}} - \frac{i_{q,i}}{i_{q,i}^{rated}}\right) \tag{9}$$

where k_q is the integral gain.

III. EVENT-TRIGGERED STRATEGY

The distributed secondary controller introduced in Section III incurs high communication traffic and, as a result, is not efficient. Conventionally, data are transmitted in a periodic way and therefor a significant amount of redundant information is exchanged, resulting in higher costs and taking up more bandwidth. To reduce the exchanged data and lighten the communication burden, an event-triggered strategy is proposed in this section. In contrast with the periodic where the DERs exchange information continuously, in the event-triggered scheme, data are transmitted at special instances referred to as event-times. Employing this strategy not only decreases the communication burden but also it lowers the costs and allows more efficient use of bandwidth. In the framework event-triggered method, the secondary controller of DER *i* is updated at its event times represented by $t_0^i, t_1^i, \dots, t_k^i$ and the event times of its neighbors defined by $t_0^j, t_1^j, \dots, t_k^j$. Hence, the (6), (8), and (9) are rewritten as:

$$\bar{v}_i = v_i(t_k^i) + \frac{k_{avg}}{s}\sum_{j\in N_i} \bar{v}_j(t_{k'}^j) - \bar{v}_i(t_k^i),\ for\ t \in \left[t_k^i, t_{k+1}^i\right) \tag{10}$$

$$r_{di}(t) = r_{do} + \frac{k_d}{s}\sum_{j\in N_i}\left(\frac{i_{d,j}(t_{l'}^j)}{i_{d,j}^{rated}} - \frac{i_{d,i}(t_l^i)}{i_{d,i}^{rated}}\right),\ for\ t \in \left[t_l^i, t_{l+1}^i\right) \tag{11}$$

$$r_{qi}(t) = r_{qo} + \frac{k_q}{s}\sum_{j\in N_i}\left(\frac{i_{q,j}(t_{m'}^j)}{i_{q,j}^{rated}} - \frac{i_{q,i}(t_m^i)}{i_{q,i}^{rated}}\right),\ for\ t \in \left[t_m^i, t_{m+1}^i\right) \tag{12}$$

in which $t_{k'}^j$, t_l^i , and t_m^i are the last events of agent *j*. The occurrence of events is decided by triggering functions. In the case of voltage, the triggering function is defined as:

$$\delta_{v,i}^2 \le \eta \frac{\alpha(1-\alpha N_i)}{N_i}\Omega_{v,i}^2 \tag{13}$$

where $\Omega_{v,i}$ is the product of Laplacian matrix (L)[17] and voltage vector ($\bar{v} = [\bar{v}_1, \bar{v}_2, \dots, \bar{v}_i]$). η and α are positive constants that meet $0<\eta<1$ and $0 < \alpha < (1/|N_i|)$ respectively. $\delta_{v,i}$ is voltage the measurement error function described as:

$$\delta_{v,i} = \bar{v}_i(t_k^i) - \bar{v}_i(t) \tag{14}$$

In analogy with voltage, triggering function for d-axis current can be defined as:

$$\delta_{id,i}^2 \le \eta \frac{\alpha(1-\alpha N_i)}{N_i}\Omega_{id,i}^2 \tag{15}$$

where $\Omega_{id,i}$ is the product of Laplacian matrix(L) and d-axis current vector ($i_d = [i_{d1}, i_{d2}, \dots, i_{di}]$) and $\delta_{id,i}$,d-axis current measurement error, is stated as:

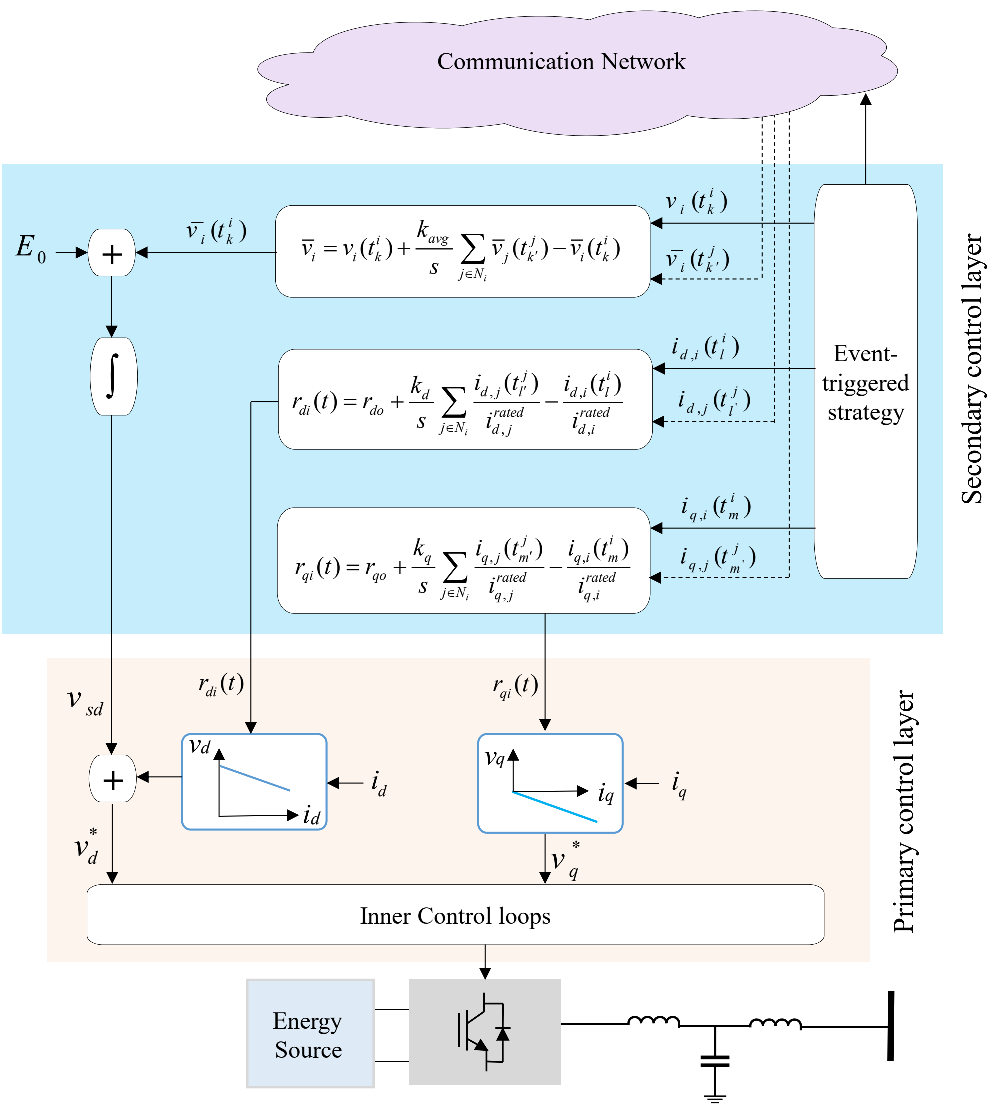

Fig. 2. Schematic diagram of the proposed control strategy

$$\delta_{id,i} = i_{di}(t_k^i) - i_{di}(t) \tag{16}$$

Similarly, q-axis current triggering function is:

$$\delta_{iq,i}^2 \le \eta \frac{\alpha(1-\alpha N_i)}{N_i}\Omega_{iq,i}^2 \tag{17}$$

In which, $\Omega_{iq,i}$ is the product of Laplacian matrix(L) and q-axis current vector ($i_q = \left[i_{q1}, i_{q2}, \ldots, i_{qi}\right]$) and $\delta_{iq,i}$,q-axis current measurement error, is:

$$\delta_{iq,i} = i_{q,i}(t_k^i) - i_{q,i}(t) \tag{18}$$

The schematic diagram of the proposed control scheme is shown in Fig. 2. The event triggered strategy determines the event times for transfer of DER data to the neighbors. By using the local measurements and neighbor information, the secondary control level computes the change in the slopes of the d and q axis droop characteristics and the offset of the d axis voltage. The primary controller computes the d and q axis components of the output voltage reference according to the vd-id and vq-iq droop characteristics. The inner control loops, which comprise of cascaded voltage and current controllers, realizes this reference voltage by controlling the PWM switching signals for the DC/AC converter. The converter's output is connected to an LCL filter, which eliminates the switching harmonics.

IV. SIMULATION RESULTS

To verify the proposed event- and self-triggered control strategies, simulation results are presented in this section. The simulations are conducted using MATLAB/Simulink. The structure of the test MG is shown in Fig. 1. The MG comprises four DERs, each of which has a rated active power of 1500W. The rated phase voltage is 220V and the rated frequency is 50Hz. The line impedances are dominantly resistive, which is in accordance with the low X/R ratio of distribution networks. Two loads (Z_{load1} and Z_{load2}) are connected to the bus 4. The communication delay is 20ms. The values of control and electrical parameters are listed in Table 1.

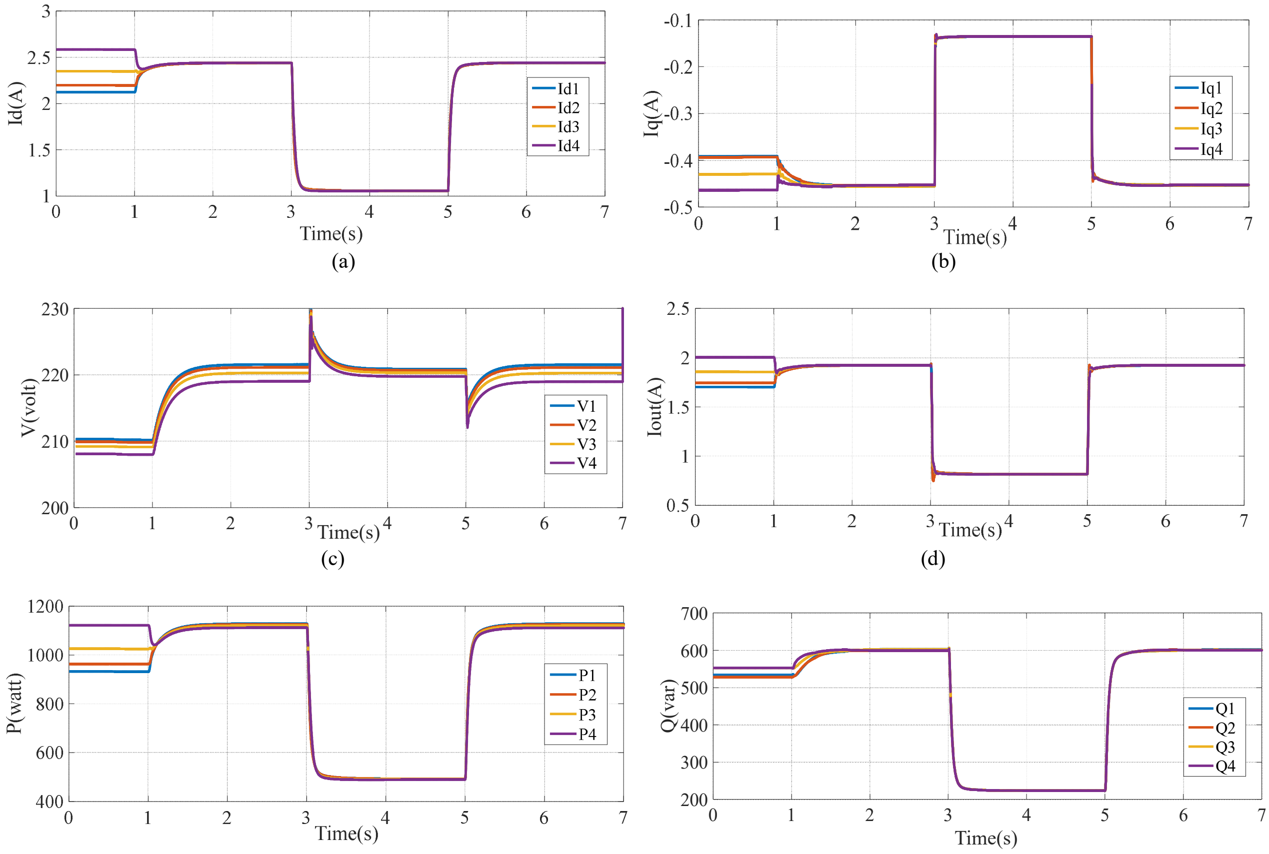

(a) (b) (c) (d) (e) (f)

Fig. 3. a) d-axis current, b) q-axis current, c) rms voltage, d) output current, e) active power, f) reactive power

Initially the secondary controller is inactive, and both of the loads are connected. Therefore, the load current is shared among the DERs in accordance with the V-I droop characteristics. Since all DERs have the same rating, it is expected that the DER provide the same d/q current outputs. However, as seen from Fig. 3(a), (b), the d and q components of the DER currents are different with the DER4 having the highest current components, followed by DER3, DER2 and DER1. This implies the presence of a current sharing error caused by the line impedances. This error reflects in the active and reactive powers of the DERs (Fig. 3 (e), (f)). Furthermore, the rms voltage of the DERs deviate from the nominal voltage by around 9-11V.

At t=1, the secondary controller is activated, and virtual impedances of d-axis and q-axis changes. Specifically, the virtual impedance of the DER4, which is closest to the loads, becomes the largest and the virtual impedance of DER1 becomes the smallest. This way, the effect of the line impedances on the load sharing is cancelled out and the current sharing error is eliminated (see Fig. 3(a), (b)). So, as shown in Fig. 3 (c), the rms output currents of the DERs also reach the same value. In addition, the average voltage of the four DERs is restored to the nominal voltage (220V). As a result, the DER terminal voltages settle within a close vicinity of the nominal voltage, as shown in Fig. 3 (c). By inspecting the Fig. 3 (e), (f), it is seen that the accurate sharing of active and reactive powers is also realized.

To investigate the dynamic response of the proposed control method to step load changes, load 2 is disconnected and connected again, at t=3s and t=5s, respectively. Subsequent to load changes, the d-axis and q-axis currents change with a fast and overshoot free transient (Fig. 3 (a) , (b)). The current changes are reflected in the output active and reactive powers (see Fig. 3 (e), (f)). Moreover, the DER voltages are restored to the nominal value after experiencing transient variations.

In order to demonstrate the advantage of the proposed event triggered strategy, the number of events for both periodic and event-triggered methods are depicted in Fig. 4. It is seen that by implementing event-triggered strategy the communication network traffic is decreased by a factor 5.

V. CONCLUSION

In this paper, a novel distributed control scheme is introduced to restore the voltage and realize accurate load sharing among the DERs in an islanded AC MG. This method comprises a primary control based on V-I droop characteristics and a secondary controller which utilizes a consensus strategy. To reduce the communication burden, an event-triggered control is applied to decrease the network traffic. MATLAB/Simulink results are provided to

Table 1. Electrical and control parameters of simulated MG

Description	**Symbol**	**Value**
Nominal phase voltage	E_0	$220\ V_{rms}$
Nominal frequency	f_r	50 Hz
Inverter nominal power	P_r	1500 W
Line impedance	Z_{L1}	0.66 + j0.07 Ω
	Z_{L2}	0.5 + j0.07 Ω
	Z_{L3}	0.5 + j0.07 Ω
Load impedance	Z_{Load1}	75 + j50.26 Ω
	Z_{Load2}	42 + j25.13 Ω
Droop coefficients	r_{do}	7
	r_{qo}	7
Secondary controller parameters	k_{avg}	1.2
	k_v	6
	k_d	80
	k_q	150
Event-Trigger parameters	α	0.125
	η	0.9
Communication delay	T_d	20 ms

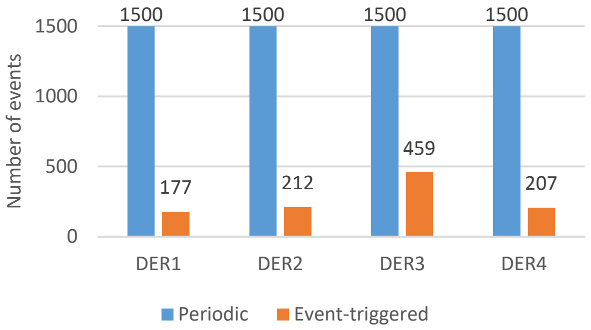

Fig. 4. Number of events in periodic and event-triggered methods

demonstrate the efficiency of the proposed method. The results show that the controller updates have been greatly reduced by a factor of 5-7 in comparison with the periodic method. Moreover, d-axis and q-axis currents are proportionally shared and voltage has been restored to the nominal value. As a result, accurate active and reactive power sharing have been achieved.

REFERENCES

[1] M. S. Golsorkhi and M. Savaghebi, "A Decentralized Control Strategy Based on V-I Droop for Enhancing Dynamics of Autonomous Hybrid AC/DC Microgrids," *IEEE Transactions on Power Electronics,* vol. 36, no. 8, pp. 9430-9440, Aug. 2021, doi: 10.1109/TPEL.2021.3049813.

[2] M. S. Golsorkhi, D. D. C. Lu, Q. Shafiee, and J. M. Guerrero, "Distributed voltage control and load sharing for inverter-interfaced microdrid with resistive lines," in *2016 IEEE Energy Conversion Congress and Exposition (ECCE)*, 18-22 Sept. 2016 2016, pp. 1-7, doi: 10.1109/ECCE.2016.7855050.

[3] Q. Shafiee, J. M. Guerrero, and J. C. Vasquez, "Distributed Secondary Control for Islanded Microgrids—A Novel Approach," *IEEE Transactions on Power Electronics,* vol. 29, no. 2, pp. 1018-1031, 2014, doi: 10.1109/TPEL.2013.2259506.

[4] M. S. Golsorkhi, D. J. Hill, and M. Baharizadeh, "A Secondary Control Method for Voltage Unbalance Compensation and Accurate Load Sharing in Networked Microgrids," *IEEE Transactions on Smart Grid,* vol. 12, no. 4, pp. 2822-2833, 2021, doi: 10.1109/TSG.2021.3062404.

[5] X. Wu and C. Shen, "Distributed Optimal Control for Stability Enhancement of Microgrids With Multiple Distributed Generators," *IEEE Transactions on Power Systems,* vol. 32, no. 5, pp. 4045-4059, 2017, doi: 10.1109/TPWRS.2017.2651412.

[6] V. Nasirian, Q. Shafiee, J. M. Guerrero, F. L. Lewis, and A. Davoudi, "Droop-Free Distributed Control for AC Microgrids," *IEEE Transactions on Power Electronics,* vol. 31, no. 2, pp. 1600-1617, 2016, doi: 10.1109/TPEL.2015.2414457.

[7] Z. Zhang *et al.*, "An Event-Triggered Secondary Control Strategy With Network Delay in Islanded Microgrids," *IEEE Systems Journal,* vol. 13, no. 2, pp. 1851-1860, 2019, doi: 10.1109/JSYST.2018.2832065.

[8] M. Chen, X. Xiao, and J. M. Guerrero, "Secondary Restoration Control of Islanded Microgrids With a Decentralized Event-Triggered Strategy," *IEEE Transactions on Industrial Informatics,* vol. 14, no. 9, pp. 3870-3880, 2018, doi: 10.1109/TII.2017.2784561.

[9] T. Qian, Y. Liu, W. Zhang, W. Tang, and M. Shahidehpour, "Event-Triggered Updating Method in Centralized and Distributed Secondary Controls for Islanded Microgrid Restoration," *IEEE Transactions on Smart Grid,* vol. 11, no. 2, pp. 1387-1395, 2020, doi: 10.1109/TSG.2019.2937366.

[10] B. Abdolmaleki, Q. Shafiee, A. R. Seifi, M. M. Arefi, and F. Blaabjerg, "A Zeno-Free Event-Triggered Secondary Control for AC Microgrids," *IEEE Transactions on Smart Grid,* vol. 11, no. 3, pp. 1905-1916, 2020, doi: 10.1109/TSG.2019.2945250.

[11] L. Ding, Q. Han, X. Ge, and X. Zhang, "An Overview of Recent Advances in Event-Triggered Consensus of Multiagent Systems," *IEEE Transactions on Cybernetics,* vol. 48, no. 4, pp. 1110-1123, 2018, doi: 10.1109/TCYB.2017.2771560.

[12] M. S. Golsorkhi and D. D. C. Lu, "A Control Method for Inverter-Based Islanded Microgrids Based on V-I Droop Characteristics," *IEEE Transactions on Power Delivery,* vol. 30, no. 3, pp. 1196-1204, 2015, doi: 10.1109/TPWRD.2014.2357471.

[13] F. Guo, C. Wen, J. Mao, and Y. Song, "Distributed Secondary Voltage and Frequency Restoration Control of Droop-Controlled Inverter-Based Microgrids," *IEEE Transactions on Industrial Electronics,* vol. 62, no. 7, pp. 4355-4364, 2015, doi: 10.1109/TIE.2014.2379211.

[14] J. W. Simpson-Porco, Q. Shafiee, F. Dörfler, J. C. Vasquez, J. M. Guerrero, and F. Bullo, "Secondary Frequency and Voltage Control of Islanded Microgrids via Distributed Averaging," *IEEE Transactions on Industrial Electronics,* vol. 62, no. 11, pp. 7025-7038, 2015, doi: 10.1109/TIE.2015.2436879.

[15] M. S. Golsorkhi and D. D. C. Lu, "A decentralized power flow control method for islanded microgrids using V-I droop," in *2014 22nd Iranian Conference on Electrical Engineering (ICEE)*, 20-22 May 2014 2014, pp. 604-609, doi: 10.1109/IranianCEE.2014.6999613.

[16] M. S. Golsorkhi and D. D. C. Lu, "A decentralized negative sequence compensation method for islanded mirogrids," in *2015 IEEE 6th International Symposium on Power Electronics for Distributed Generation Systems (PEDG)*, 22-25 June 2015 2015, pp. 1-7, doi: 10.1109/PEDG.2015.7223019.

[17] M. S. Golsorkhi, Q. Shafiee, D. D. Lu, and J. M. Guerrero, "Distributed Control of Low-Voltage Resistive AC Microgrids," *IEEE Transactions on Energy Conversion,* vol. 34, no. 2, pp. 573-584, 2019, doi: 10.1109/TEC.2018.2878690.